Forward coupling phenomena between artificial left-handed transmission lines

Lei Liu,[a] Christophe Caloz, Chin-Chang Chang, and Tatsuo Itoh
Department of Electrical Engineering, University of California, Los Angeles, California 90095

(Received 29 April 2002; accepted 14 August 2002)

Coupling phenomena between artificial left-handed (LH) transmission lines are explored on the basis of a transmission line approach of LH materials. A LH forward coupler in the form of an ideal lumped-element ladder network is presented and is shown to exhibit strong forward coupling that increases with decreasing of frequency. A quasi-lumped element microstrip implementation of a LH coupler is proposed. It is demonstrated that this coupler requires a shorter coupling length in comparison with the conventional right-handed coupled-line forward couplers, and hence makes the device much more compact. © *2002 American Institute of Physics.* [DOI: 10.1063/1.1512682]

I. INTRODUCTION

In 1968, Veselago performed the first theoretical investigation of left-handed (LH) materials, which are characterized by simultaneous negative permittivity and permeability.[1] After his publication, the possible creation of such materials was repeatedly discussed in the literature.[2–4] Recently, Smith *et al.*[5] and J. B. Pendry *et al.*[6] demonstrated the practical realization of LH materials with split-ring resonators and thin-wire structures. From then on, there has been an increasing interest in LH materials and their potential applications.

A variety of optical applications, based on the properties of LH materials such as reversal of Snell's law, Doppler effect, and Cerenkov radiation, have been proposed.[7,8] However, the structures presented so far are not suitable for practical microwave applications, because of their excessive loss and narrow bandwidth. Caloz *et al.* introduced a transmission line (TL) approach of LH materials and proposed an artificial LH transmission line with microstrip components including interdigital capacitors and shorted stub inductors.[9] This transmission line approach has shown that LH structures can present moderate insertion loss and broad bandwidth, which suggests that their properties may be used efficiently in microwave applications.

Conventional coupled-line forward couplers can achieve strong forward coupling, but their drawback is that they require very long physical lengths and very tight spacing between the two lines to attain a sufficient coupling level.[10,11] In this article, we explore forward coupling phenomena between artificial LH transmission lines and propose a microstrip implementation of a forward LH coupler using quasi-lumped elements, and demonstrate that the coupling length of this LH forward coupler can be drastically reduced in comparison to that of the conventional coupler.

II. THE PRINCIPLE OF REALIZATION OF A LH COUPLER

Forward couplers are widely used in different microwave circuits and systems. Therefore, coupling effects between LH transmission lines represent an interesting research topic, which may lead to new types of couplers along with new applications for LH materials. In Ref. 9 an electrical dual circuit of the conventional right-handed (RH) transmission line is presented, in which the per-unit-length inductance and capacitance is exchanged [see Fig. 1(a)]. The corresponding propagation constant is

$$\beta(\omega) = -1/(\omega\sqrt{LC}), \tag{1}$$

which yields the phase velocity $v_p = -\omega^2\sqrt{LC} < 0$ and group velocity $v_g = +\omega^2\sqrt{LC} > 0$, as shown in Fig. 1(b). The characteristic impedance of this transmission line is the same as that of RH lines: $Z_c = \sqrt{L/C}$. By equating the admittances of this line, $Z' = 1/(j\omega C')$ and $Y' = 1/(j\omega L')$ to those of a corresponding material, $Z' = j\omega\mu$ and $Y' = j\omega\epsilon$, the equivalent material parameters take the form $\epsilon(\omega) = -1/(\omega^2 L)$ and $\mu(\omega) = -1/(\omega^2 C)$, and are seen to be simultaneously negative and dispersive. Finally, the equivalent index of refraction is derived by taking the square root of the product of $\epsilon(\omega)$ and $\mu(\omega)$, which yields $n(\omega) = -c_0/(\omega^2\sqrt{L'C'}) < 0$. The negativity of equivalent material parameters and index of refraction indicate the LH nature of this transmission line.

In the transmission line approach, a single LH line with arbitrary per-unit-length series capacitance (C') and parallel inductance (L') can be realized in the form of an artificial lumped-element ladder network obtained by repeating N unit cells comprised of a series capacitor (C_u) and a shunt inductor (L_u). Practically, in order to obtain a good approximation at a given frequency f, the unit length $P_u = P/N$ should satisfy $P_u < \lambda_g/10$, which yields

$$N > \frac{10P}{(2\pi)^2\sqrt{L'C'}f} = N_{\min}(f), \tag{2}$$

and C_u, L_u are given by

$$C_u = C' \cdot N/P, \qquad L_u = L' \cdot N/P. \tag{3}$$

The valid frequency range of this approximation is then

[a]Electronic mail: liulei@ee.ucla.edu

 © 2002 American Institute of Physics

Downloaded 25 Jun 2003 to 128.97.11.57. Redistribution subject to AIP license or copyright, see http://ojps.aip.org/japo/japcr.jsp

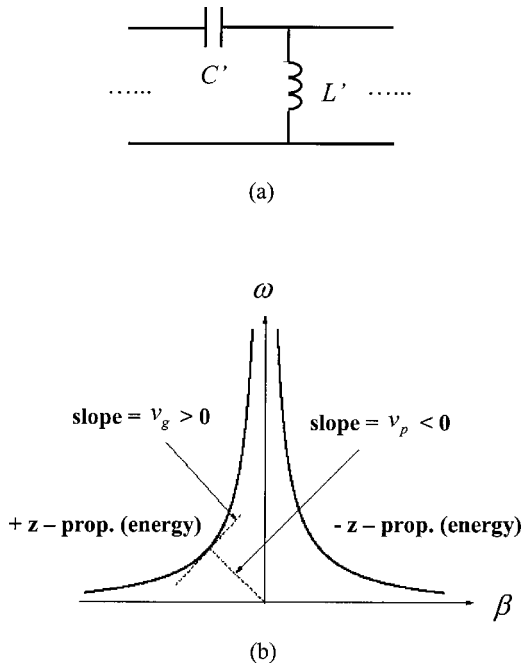

FIG. 1. LH transmission line. (a) Infinitesimal circuit model of the LH transmission line as the dual of the conventional transmission line. (b) ω–β diagram of the LH transmission line.

$$f > \frac{10P}{(2\pi)^2\sqrt{L'C'N}} = \frac{10}{(2\pi)^2\sqrt{L_uC_u}} = \int_{\min}^{approx} \tag{4}$$

As frequency decreases, the accuracy of the approximation degrades down to the cutoff frequency,

$$f_c = 1/(4\pi\sqrt{L_uC_u}), \tag{5}$$

where no wave can propagate. The artificial LH transmission line is therefore a high-pass filter. Figure 2(a) shows a physical representation of the LH coupler, which consists of two parallel LH transmission lines with physical length P and separation distance S. For this four-port network, the even and odd mode S-parameters S_{11e}, S_{11o}, S_{22e}, and S_{22o} should satisfy $S_{11e}=S_{11o}=S_{22e}=S_{22o}$.[11] Practically, this condition can be nearly met by keeping a relatively large spacing between the transmission lines. The equivalent circuit model of the coupler is shown in Fig. 2(b). The mutual capacitance for the unit-cell, C_{mu}, is given by

$$C_{\mathrm{mu}} = C_{\mathrm{tot}}/N, \tag{6}$$

where C_{tot} is the total value of mutual capacitance between two LH lines and is determined by physical parameters, such as the separation between two lines and substrate characteristics. The following procedure can be used to mimic a fictitious LH forward coupler using the circuit model shown in Fig. 2(b). First, for a physical length P, arbitrary per-unit-length capacitance and inductance and given frequency f, determine the minimum number of cells N required to satisfy Eq. (2). Second, calculate the unit cell element values C_u, L_u using Eq. (3). Third, the value of unit-cell mutual capacitance C_{mu} is calculated from the detailed physical structure.

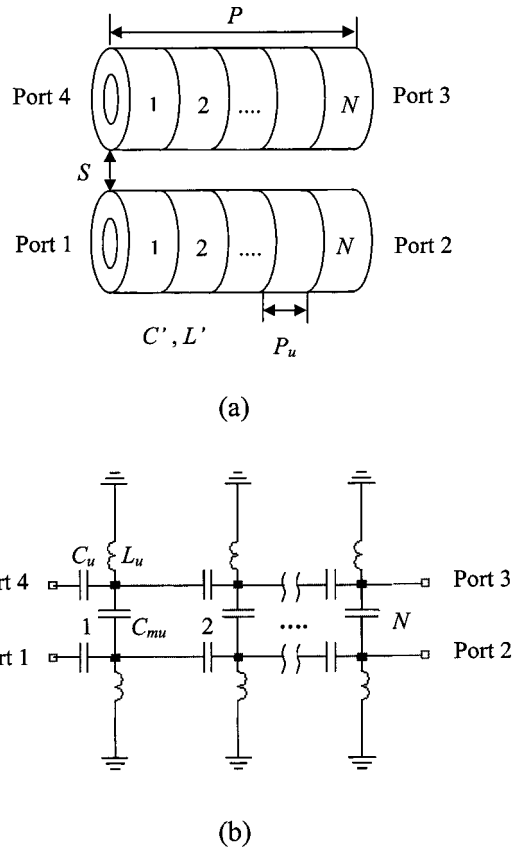

FIG. 2. LH forward coupler. (a) Physical representation with fictitious LH transmission lines. (b) Equivalent circuit model.

III. ANALYSIS OF LH FORWARD COUPLER

Due to the symmetry of the LH coupler, the circuit model introduced in the previous section is analyzed using even-odd mode decomposition technique.[11] This technique makes use of the physical symmetry of this LH forward coupler. By applying symmetric (even mode) and antisymmetric (odd mode) excitation to two ports of the circuit model, the four-port problem is reduced to that of solving two two-port problems. The two two-port problems to be analyzed are shown in Fig. 3. For even and odd modes, the unit-cell $[ABCD]$ matrix M_{ue} and M_{uo} can be expressed in terms of C_u, L_u, and C_{mu} as[12]

$$M_{ue} = \begin{bmatrix} 1 - 1/\omega^2 L_u C_u & 1/j\omega C_u \\ 1/j\omega L_u & 1 \end{bmatrix} \tag{7}$$

and

$$M_{uo} = \begin{bmatrix} \dfrac{\omega^2 L_u(2C_{\mathrm{mu}} + C_u) - 1}{\omega^2 LC} & 1/j\omega C_u \\ (1 - 2\omega^2 L_u C_{\mathrm{mu}})/j\omega L_u & 1 \end{bmatrix}. \tag{8}$$

The two-port $[ABCD]$ matrix M_e for even mode and M_o for odd mode can be obtained by cascading these unit-cell matrixes, $M_e = M_{ue}^N$ and $M_o = M_{uo}^N$. The two-port S-parameters become

$$\Gamma_e(S_{11e}) = \frac{A_e + B_e/Z_0 - C_e Z_0 - D_e}{A_e + B_e/Z_0 + C_e Z_0 + D_e},$$

Downloaded 25 Jun 2003 to 128.97.11.57. Redistribution subject to AIP license or copyright, see http://ojps.aip.org/japo/japcr.jsp

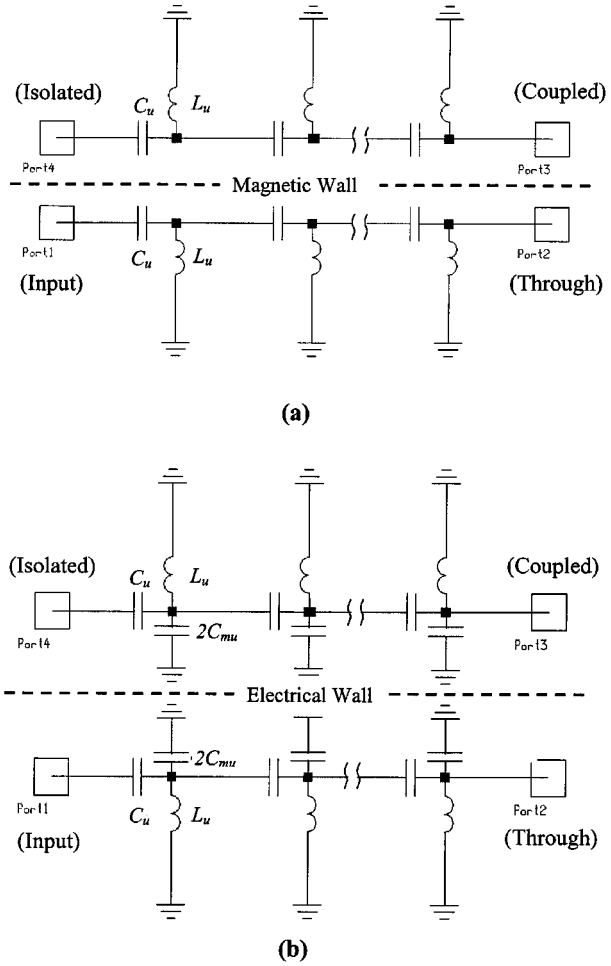

FIG. 3. Equivalent circuit model. (a) Even mode with magnetic wall. (b) Odd mode with electrical wall.

$$T_e(S_{21e}) = \frac{2}{A_e + B_e/Z_0 + C_e Z_0 + D_e},$$
$$\Gamma_o(S_{11o}) = \frac{A_o + B_o/Z_0 - C_o Z_0 - D_o}{A_o + B_o/Z_0 + C_o Z_0 + D_o}, \tag{9}$$
$$T_o(S_{21o}) = \frac{2}{A_o + B_o/Z_0 + C_o Z_0 + D_o}.$$

In Eq. (9), Γ_e T_e and Γ_o T_o represent the even and odd mode transmission and reflection coefficients, respectively. Finally the four-port S parameters can be calculated by

$$S_{11} = \tfrac{1}{2}\Gamma_e + \tfrac{1}{2}\Gamma_0, \quad S_{21} = \tfrac{1}{2}T_e + \tfrac{1}{2}T_o,$$
$$S_{31} = \tfrac{1}{2}T_e - \tfrac{1}{2}T_o, \quad S_{41} = \tfrac{1}{2}\Gamma_e - \tfrac{1}{2}\Gamma_0. \tag{10}$$

We can apply this circuit model to describe the coupling effects between two identical fictitious LH lines with parameters $P = 285$ mm, $C' = 0.033$ pF m, $L' = 0.059$ nH m. From Eq. (2), to obtain good approximation accuracy at frequencies larger than $f_{\min}^{\text{approx}} \approx 4$ GHz, we must have $N = 13$, then $C_u = 1.50$ pF, $L_u = 2.69$ nH following Eq. (3). For the mutual capacitance, however, we lack the physical structure information for fictitious LH lines. Therefore, as a first attempt, we assume that the total value of mutual capacitance between two LH lines is equal to that of RH lines with the same physical length, which yields here $C_{\text{mu}} = 0.14$ pF. The resulting S parameters of this four-port network are shown in Fig. 4. In Fig. 4(a), the coupling parameter S_{31} is close to 0 dB at about $f_0 = 5$ GHz, where S_{21}, S_{11}, and S_{41} are all below -20 dB. This demonstrates that complete forward coupling of energy from port 1 to port 3 is achieved at this frequency. As the frequency decreases, S_{31} decreases and S_{21} increases. Below 4 GHz, the approximation accuracy is insufficient, and the 1.25 GHz cutoff frequency shows the high-pass nature of the structure. In Fig. 4(b), the number of cells is increased to 20, which yields a good approximation above $f_{\min}^{\text{approx}} \approx 2.6$ GHz by Eq. (4). Thus, in Fig. 4(b), besides the complete coupling phenomenon existing at 5.0 GHz, -3 dB forward coupling is observed at 2.8 GHz with potential applications for power dividers. The input energy here is

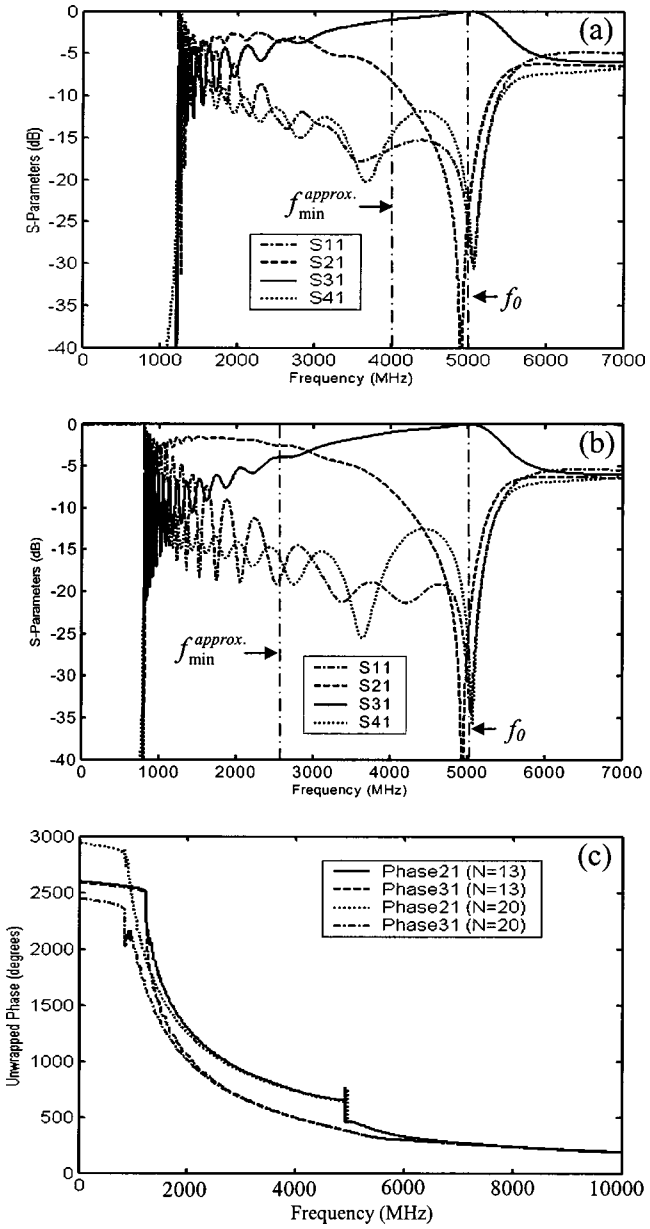

FIG. 4. Even-odd mode analysis of ideal lumped element model for LH forward coupler. (a) S-parameters of $N = 13$. (b) S-parameters of $N = 20$. (c) Unwrapped phase of S-parameters.

Downloaded 25 Jun 2003 to 128.97.11.57. Redistribution subject to AIP license or copyright, see http://ojps.aip.org/japo/japcr.jsp

equally divided by port 2 and port 3. Correspondingly, C_u, L_u change to $C_u = 2.32$ pF, $L_u = 4.14$ nH, according to Eq. (3). To keep the same total value of mutual capacitance between two LH lines, the unit-cell mutual capacitance is changed to be $C_{\mathrm{mu}} = 0.09$ pF, using Eq. (6). The cutoff frequency moves to a lower frequency of 0.81 GHz following Eq. (5). When the number of cells N tends to infinity, the cutoff frequency tends to zero and a perfect LH forward coupler is realized. At frequencies higher than 6 GHz, all four S parameters tend to -6 dB, indicating that power is equally divided among the four ports. This phenomenon can be explained by the circuit model itself, in which the capacitances become short and the inductance becomes open at high frequencies.

In order to further identify the left-handedness of this forward coupler, the phases of S_{31} and S_{21} have been unwrapped in Fig. 4(c), which represents the ω–β diagram of the coupler. According to the transmission line theory of LH materials, the expression of propagation constant $\beta(\omega) = -1/(\omega\sqrt{LC})$ shows that $\lambda(\omega) = 2\pi/\beta(\omega)$ is proportional to ω, and not to $1/\omega$ as in a RH-TL. Thus the phase of the transmitted signal is zero at infinite frequency where it is the open-circuit point in the Smith Chart.[13] It rotates counterclockwise as frequency decreases. At zero frequency, the cumulated phase tends to infinity while the cutoff frequency approach zero with increasing N. Figure 4(c) demonstrates that the ω–β diagrams of S_{31} and S_{21} show strong left-handedness.

For a conventional coupled-line forward coupler $\beta \propto \omega$, the guided wavelength $\lambda_g = 2\pi/\beta$ is proportional to $1/\omega$, and the electrical length $P_e = P/\lambda_g$ is therefore proportional to ω. When frequency is increased, the electrical length becomes larger and the coupling level eventually reaches a maximum at a given physical length. Thus, in order to obtain maximum forward coupling, we need either a long physical length or a high frequency. In contrast, in the LH forward coupler, $\beta \propto 1/\omega$, as can be seen in Fig. 4(c). Consequently, $\lambda_g \propto \omega$ and $P_e \propto 1/\omega$. The electrical length is zero at infinity, and the forward coupling effect becomes larger and larger as frequency *decreases* and then reaches a maximum. Thus, it is easier to achieve strong forward coupling at lower frequencies for LH couplers.

Another merit of this kind of forward coupler is that the values of the lumped elements will decrease with the reduction of number of cells according to Eq. (3). In order to obtain total coupling at a given frequency f_0, we only need good approximation above a frequency $f_{\min}^{\mathrm{approx}}$ which is a little bit lower than f_0 and yields a minimum number of cells according to Eq. (2). For example, in Fig. 4, if we only need to obtain strong forward coupling at $f_0 = 5$ GHz, the number of cells of this circuit can be reduced further. For instance, let $f_{\min}^{\mathrm{approx}} \approx 5$ GHz and then $N = 10$ is enough. As shown in Table I, with decreasing of N, the values of C_u, L_u decrease to $C_u = 1.15$ pF, $L_u = 2.07$ nH that are much smaller than when N is larger. For two- or three-dimensional (3D) implementation, this kind of coupler has great potential to reduce size while keeping the same performance at the given coupling frequency.

TABLE I. Data comparison of ideal lumped-element circuit model for LH couplers with different number of cells.

Number of cells	C_u (pF)	L_u (nH)	C_{mu} (pF)	$f_{\min}^{\mathrm{approx}}$ (GHz)	f_c (GHz)
20	2.32	4.14	0.09	2.6	0.81
13	1.50	2.69	0.14	4.0	1.25
10	1.15	2.07	0.18	5.0	1.62

IV. MICROSTRIP IMPLEMENTATION OF LH COUPLER

A. Physical structure

We have demonstrated in the previous section the possibility of achieving strong forward coupling with artificial LH transmission lines realized with ideal lumped-element capacitors and indictors. The potential of LH coupler to reduce the device size has also been indicated. Although this kind of forward coupler can be best realized with chip components, such as Surface-Mount Technology (SMT) capacitors and indictors, we propose here a microstrip implementation of the LH coupler with quasi-lumped component elements using inter-digital capacitors and shorted stub indictors, because of the potential of microstrip structures to be extended to real 2D and 3D artificial LH ''materials.''

Figure 5(a) shows a picture of the LH coupler prototype (6-cell, $N = 6$) fabricated on a commercial substrate RT/Duroid 5880 with a relative dielectric constant $\epsilon_r = 2.2$ and a thickness $h = 1.57$ mm. The layout for a unit cell is shown in Fig. 5(b), where the interdigital capacitor has 10 fingers, each of which is 9.8 mm long and 0.3 mm wide, and spaced by 0.2 mm with respect to the adjacent ones. The stub in each cell is 2.0 mm in width and 9.9 mm in length as shown in Fig. 5(b), and is shorted through a via to ground. The C/L values are $C_u = 2.06$ pF, $L_u = 4.62$ nH at 1.5 GHz, which

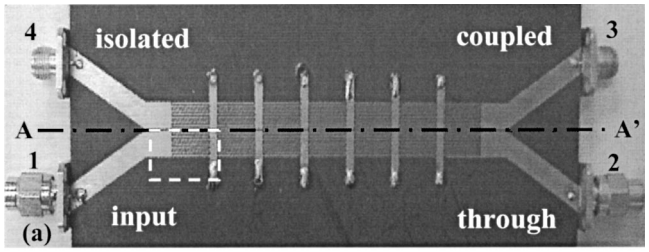

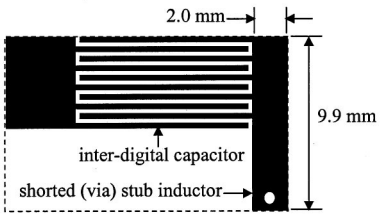

(b)

FIG. 5. Microstrip implementation of LH forward coupler (6-cell). (a) Picture of the LH coupler realized with microstrip quasi-lumped elements. (b) Layout of the unit cell.

Downloaded 25 Jun 2003 to 128.97.11.57. Redistribution subject to AIP license or copyright, see http://ojps.aip.org/japo/japcr.jsp

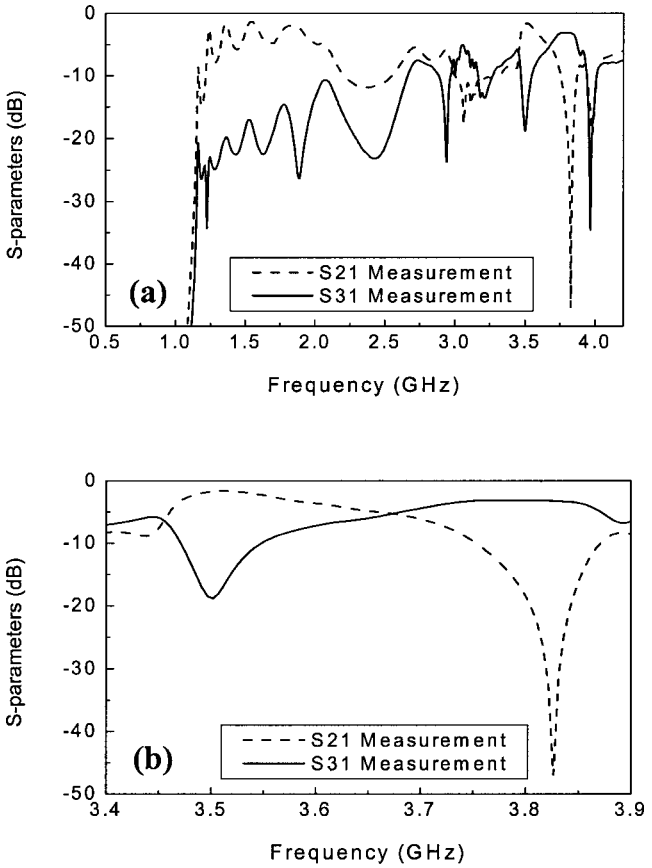

FIG. 6. Measurement results for LH forward coupler. (a) Measured S-parameters: S21 and S31. (b) Exploded S-parameters from 3.4–3.9 GHz.

yields the cutoff frequency $f_c \approx 1.1$ GHz. In this structure, the two artificial LH transmission lines with port numbers as shown in Fig. 5(a) are uniform and symmetric about the line AA'. The separation between two lines is $S=0.2$ mm. According to the realization principle of a LH coupler discussed in Sec. II, the microstrip structure presented here represents the coupling effect between two LH transmission lines with parameters $P=90$ mm, $C'=0.033$ pF m, $L'=0.059$ nH m. The value of mutual capacitance for one cell is roughly given by[12]

$$C_{\mathrm{mu}} \approx \frac{\pi \epsilon_{r_{\mathrm{eff}}} \epsilon_0 l}{N \cdot \ln\left(\frac{\pi S}{w+t}+1\right)}(F). \tag{11}$$

In Eq. (11), w and t are the width and the thickness of the conductor, respectively. The effective dielectric constant of the substrate is $\epsilon_{r_{\mathrm{eff}}}$. The coupling length of the coupler is l and the separation between the two artificial LH transmission lines is S. Based on the even-odd mode decomposition technique proposed in Sec. III, this LH coupler with above parameters N, C_u, L_u, and C_{mu} will achieve total forward coupling at about 2 GHz.

B. Measurement results

Figure 6(a) shows the S-parameters of the LH forward coupler measured with an Agilent-8510C network analyzer.

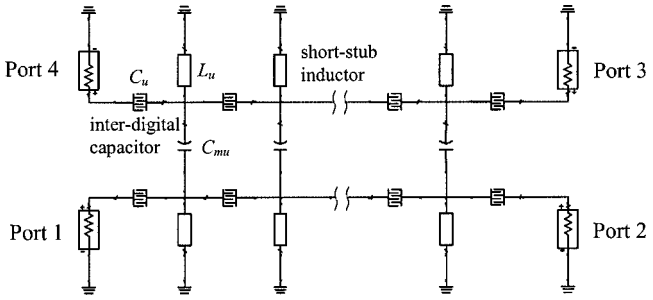

FIG. 7. ADS quasi-lumped element circuit model for 6-cell LH forward coupler.

First, S_{31} and S_{21} demonstrate that the LH transmission lines and the LH coupler are essentially high-pass filters, with a cutoff frequency of about 1.1 GHz, which is same as that of each LH line isolated. Second, a strong forward coupling at the frequency 3.83 GHz is observed. Almost all the power is transferred from port 1 to port 3. At 3.5 GHz, almost all the power is transferred from port 1 to port 2, and at 3.66 GHz, the power is equally divided by port 2 and port 3.

C. Discussion and comparison

The inductance value used in this structure is obtained from $L_u(\omega)=(Z_0^{\mathrm{stub}}/\omega)\cdot \tan(\omega l\sqrt{\epsilon_e}/c_0)$. Therefore, the inductance provided by the shorted stub has an absolute high-frequency limit $f_{\mathrm{up}}=\pi c_0/(4l\sqrt{\epsilon_e})$, above which the shorted stub becomes a capacitor. The interdigital capacitors are also

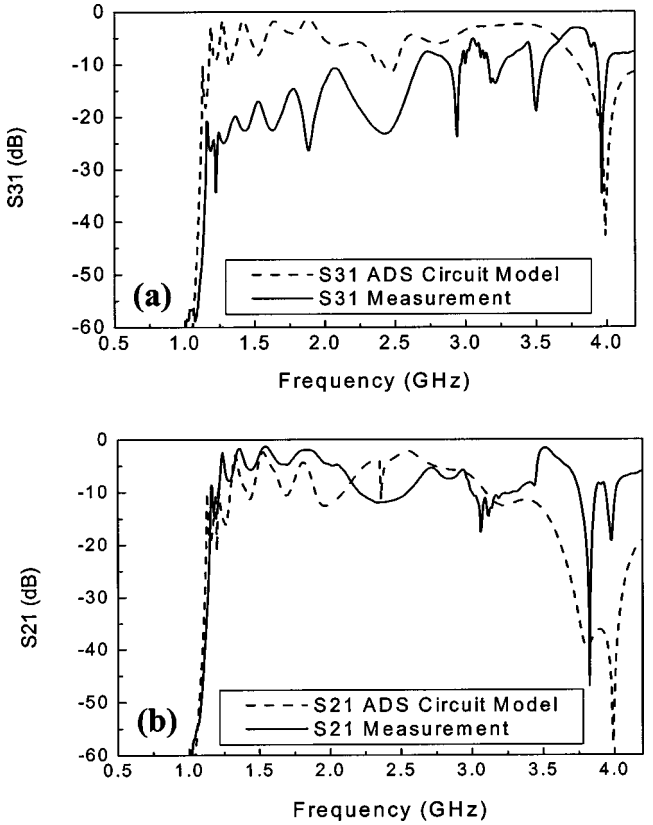

FIG. 8. Comparison between the simulation results and measurement results. (a) S31 (b) S21.

Downloaded 25 Jun 2003 to 128.97.11.57. Redistribution subject to AIP license or copyright, see http://ojps.aip.org/japo/japcr.jsp

TABLE II. Comparison between LH forward coupler and conventional coupler fabricated on same substrate with same separation distance.

	LH forward coupler	Conventional coupler	Conventional coupler
S (mm)	0.2	0.2	0.1
P (mm)	90	370	340

Substrate: RT/Duroid 5880 with $\varepsilon_r = 2.2$ and $h = 1.57$ mm. Maximum forward coupling: 3.85 GHz.

dispersive. According to full-wave simulations, the interdigital capacitor starts to resonate at about 4.0 GHz, which limits the usable bandwidth. The dispersive nature of the interdigital capacitors and shorted inductors will necessarily introduce some discrepancy with respect to the ideal lumped-element model. Therefore, in addition to having a cutoff frequency limit, this microstrip implementation of LH forward coupler also has a high frequency limit imposed by the dispersive nature of the C/L components. Considering the differences between the ideal lumped element model and the microstrip implementation circuits, we need to analyze the latter more accurately. The full-wave analysis methods, such as the finite difference time domain and the Method of Moments are too time-consuming because of high complexity of this structure. The widely used software Advanced Design System (ADS) provides microstrip quasi-lumped elements such as interdigital capacitors and stub inductors so that we can develop a circuit model with these components. The quasi-lumped element circuit model we constructed is shown in Fig. 7. The dimensions of the interdigital capacitors and shorted stub inductors in the ADS circuit model are same as those of the physical structure.

Figure 8 shows the comparison between the simulation results and measurement. The cutoff frequency of the measured curves agrees with the simulation results. In addition, the general shape of the simulation curves and the measured curves are roughly comparable. The measured curves display larger losses than simulation results, essentially because of reflections (mismatch) between the different circuit elements. The structure proposed here has a physical length of about 90 mm. We compare its performances to a conventional RH coupled line forward coupler with the same substrate and the same separation distance. The width of the single microstrip transmission line is 4 mm to achieve 50 ohm characteristic impedance. In order to achieve maximum forward coupling at 3.83 GHz, the physical length of this RH forward coupler will be as long as 370 mm. Even by placing the two lines closer, the physical length of this coupler can not be reduced effectively. Table II lists the dimensions needed to achieve maximum forward coupling at 3.83 GHz using a LH forward coupler compared to using a conventional RH forward coupler. Considering the loss from metal, substrate, and connectors, to get maximum forward coupling, the size of the LH transmission line forward coupler is greatly reduced compared to an RH one.

V. CONCLUSION

In this article, the coupling phenomena between LH transmission lines have been explored. By analyzing the phenomena with a circuit model and even-odd mode decomposition technique, we have demonstrated the possibility of achieving strong forward coupling with LH transmission lines. A new type of forward wave directional coupler with reduced size but moderate loss and excellent directivity realized with microstrip component elements based on the transmission line approach of LH materials has been introduced. This microstrip implementation of LH transmission lines and forward couplers might be extended to 2D and 3D ''real LH materials'' in the microwave range, and lead to novel applications for LH materials.

ACKNOWLEDGMENT

This work is part of the MURI program ''Scalable and Reconfigurable Electromagnetic Metamaterials and Devices.'' It is supported by the Department of Defense (N00014-01-1-0803) and monitored by the U.S. Navy/Office of Naval Research.

[1] V. G. Veselago, Sov. Phys. Usp. **10**, 509 (1968).
[2] A. N. Lagarkov and A. K. Sarychev, Phys. Rev. B **53**, 6318 (1996).
[3] M. V. Kostin and V. V. Shevchenko, Radiotekh. Elektron. (Moscow) **11**, 1652 (1992).
[4] A. N. Lagarkov, V. N. Semenenko, V. A. Chistyaev, D. E. Ryabov, S. A. Tretyakov, and C. R. Simovski, Electromagnetics **17**, 213 (1997).
[5] D. R. Smith, W. J. Padilla, D. C. Vier, S. C. Nemat-Nasser, and S. Schultz, Phys. Rev. Lett. **84**, 4184 (2000).
[6] J. B. Pendry, A. J. Holden, D. J. Robbins, and W. J. Stewart, J. Phys.: Condens. Matter **10**, 4785 (1998).
[7] J. B. Pendry, Phys. Rev. Lett. **85**, 3966 (2000).
[8] Z. M. Zhang and C. J. Fu, Appl. Phys. Lett. **80**, 1097 (2002).
[9] C. Caloz, H. Okabe, T. Iwai, and T. Itoh, USNC/URSI National Radio Science Meeting, San Antonio, TX, June, 2002.
[10] C.-C. Chang, Y. Qian, and T. Itoh, *IEEE MTT-S International Microwave Symposium Digest*, Phoenix, AZ, May, 2001.
[11] R. Mongia, I. Bahl, P. Bhartia, *RF and Microwave Coupled-Line Circuits* (Artech House, Boston, 1999).
[12] C. S. Walker, *Capacitance, Inductance and Crosstalk Analysis* (Artech House, Boston, 1990).
[13] David M. Pozar, *Microwave Engineering* (Wiley, 1998).

Downloaded 25 Jun 2003 to 128.97.11.57. Redistribution subject to AIP license or copyright, see http://ojps.aip.org/japo/japcr.jsp